# Non Contiguous Frequency Hopping Aided OFDM-DCSK Design Without Requiring CSI

Zhaofeng Liu<sup>1</sup>, Lin Zhang<sup>12</sup>, *Member, IEEE*, Zhiqiang Wu<sup>34</sup>, *Senior Member, IEEE*<sup>1</sup>School of Electronics and Information Technology, Sun Yat-sen University, Guangzhou, 510006, China

<sup>2</sup>Guangdong Provincial Key Laboratory of Information Security Technology, Guangzhou, 510006, China

<sup>3</sup>Department of Electrical Engineering, Tibet University, Lasa, 850012, China

<sup>4</sup>Department of Electrical Engineering, Wright State University, Dayton, 45435, United States

E-mail: isszl@mail.sysu.edu.cn

Abstract-In this paper, we present a frequency hopping (FH) orthogonal frequency division multiplexing-aided differential chaos shift keying (OFDM-DCSK) modulation system for cognitive radio (CR) systems operating over non contiguous bands. Our aim is to provide reliable transmissions for CR transceivers which may hardly get the exact and perfect channel state information (CSI). In our design, we utilize the natural high security of chaotic sequences and the frequency diversity brought by the FH. The information bits are firstly modulated by chaotic chips, then both reference chips and chaotic modulated symbols are carried out FH operations and hopped non-repetitively. After performing the inverse fast Fourier transform (IFFT) over available non-contiguous spectrum bands, the resultant OFDM symbols are transmitted and the non-repetitive reference chips are respectively transmitted over different subcarriers. Subsequently, the receiver would retrieve the information using the received reference chaotic chips which naturally embed the channel frequency response (CFR) of all subcarriers. The bit error rate (BER) expressions are derived and simulations results verify the effectiveness of our derivations, which demonstrate that the presented system can achieve better BER than counterpart systems, especially when the CSI is not exact or unknown.

*Index Terms*—Bit error rate; channel state information; differential chaos shift keying; frequency hopping; non-contiguous bands; orthogonal frequency-division multiplexing.

# I. INTRODUCTION

In order to meet the increasing demands for the data rate of end users, the carrier aggregation (CA) technology has been employed by the 3rd Generation Partnership Project (3GPP) Long Term Evolution-Advanced (LTE-A) to aggregate the available bandwidth for transmissions [1]. Moreover, the cognitive radio (CR) technology can be utilized to identify available spectrum holes in the licensed spectrum to allow the transmissions over the unused or underutilized sub-bands without bringing interferences to primary users [2], [3].

In CR or CA systems, the aggregated contiguous or noncontiguous (NC) bands can provide more bandwidths, however, due to the possible discontinuity of specific bands, the receivers may not get the exact channel state information (CSI). Moreover, due to the broadcasting property of wireless channels, the CA and CR systems may suffer from the eavesdropping or the malicious attacks.

The chaotic sequence have been used to provide high security transmissions thanks to non-periodic, noise-like and sensi-

tive to initial value properties [4] [5]. Compared with coherent chaotic modulations, the non-coherent differential chaos shift keying [6] (DCSK) has attracted more research interests due to the removal of complex chaotic synchronization circuits, and the bit error rate (BER) rate performance can meet the user demands [7] even when no channel estimation is available. However, the DCSK scheme has two main drawbacks [7]: one drawback is the low efficiency since the information-bearing symbols are delivered in only half of the DCSK symbol duration and another one is that the delay line used in the modulator is difficult to be implemented in practical circuits.

Multi-carrier (MC) transmission such as the orthogonal frequency-division multiplexing (OFDM) schemes have been applied in DCSK systems [8] [9] to address the issues of the low efficiency and the delay line. However, OFDM-DCSK systems require to get exact CSI since receivers have to evaluate the channel frequency response (CFR) when we transmit the information over frequency selective fading channels [10]. [11], [12] present that the DCSK systems can achieved satisfactory BER performances over frequency selective Rayleigh fading channel without CSI, thanks to the high auto-correlation value and low cross-correlation value of chaotic sequences. However, few researches have been done on improving the performances for OFDM-DCSK CR or CA systems which may not obtain the exact CSI.

In this paper, we propose a non contiguous frequency hopping OFDM-DCSK (NC-FH-OFDM-DCSK) modulation scheme not requiring CSI. Different from conventional schemes, the hopping operations are carried out to distribute chaotic chips of chaotic sequences to different subcarriers and different time slots before inverse fast Fourier transform (IFFT) at the transmitter.

At the transmitter, after the serial to parallel (S/P) conversion, the information is modulated by chaotic chips. Then the reference chaotic chips and the chaotic modulated symbols randomly hop in different time slots and over different subcarrier. After the hopping, all chaotic chips of one chaotic sequence are distributed over all subcarriers. At the receiver, the correlation demodulation performed on different sequences can be applied with full frequency diversity since the CFR of frequency selective Rayleigh fading channel can be automatically counteracted.

The main contributions include: 1)we present a frequency hopping OFDM-DCSK scheme to improve the BER performance, and no perfect CSI is required for information recovery; 2)different from the conventional OFDM-DCSK [9], the presented NC-FH-OFDM-DCSK scheme can work well in the CR or CA systems operating over NC bands; 3)we derive the theoretical BER expressions over the additive white Gaussian noise (AWGN) channel and the frequency selective Rayleigh fading channels.

The rest of the paper is organized as follows. : Section II presents the NC-FH-OFDM-DCSK design, then Section III gives the theoretical BER analysis. Simulations are provided in Section IV. Finally, Section V concludes this paper.

# II. THE NC-FH-OFDM-DCSK DESIGN

In this section, we provide the details of the presented NC-FH-OFDM-DCSK scheme, including the transceiver structure, hopping and de-hopping modules.

# A. NC-FH-OFDM-DCSK Transmitter Structure

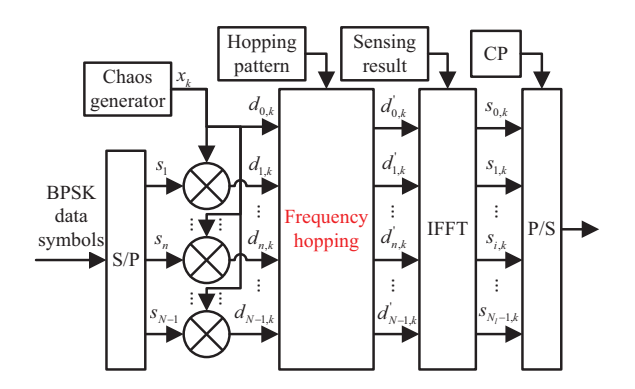


Fig. 1. The NC-FH-OFDM-DCSK transmitter structure.

Fig. 1 illustrates the NC-FH-OFDM-DCSK transmitter. The user data are firstly modulated by the binary phase shift keying (BPSK) scheme, then after the S/P conversion, the BPSK data symbols are modulated by the chaotic sequences output from the chaos generator. Subsequently, both the reference chaotic chips and the chaotic modulated symbols hop randomly in the frequency domain in the frequency hopping module. The resultant symbols are then input to the IFFT module to construct the OFDM symbols. After adding the cyclic prefix (CP) and parallel to serial (P/S) conversion, these symbols are transmitted over the channels.

Specifically, in the chaos generator, we employ the second order Chebyshev polynomial function (CPF) to generate the chaotic sequences of length  $\beta$ . Namely, the reference chaotic sequence is generated by  $x_{k+1}=1-2x_k^2$  and  $0 \le k \le \beta-1$ , where  $-1 < x_k < 1$  denotes the kth chip of the chaotic sequence and the initial number  $x_0$  can be set as 0.1.

The resultant reference chaotic sequences are then used to modulate user data, followed by the frequency hopping and IFFT operations to be detailed as below.

1) Chaotic modulation: Let  $s_n$  denote the nth  $(n = 1, 2, \dots, N-1)$  BPSK data symbol. We modulate the  $s_n$  with

the kth chaotic chip, the resultant information-bearing chaotic modulated symbol  $d_{n,k}$  is expressed as

$$d_{n,k} = s_n x_k. (1)$$

Notably, for the sake of brevity to express the data input to the frequency hopping module, we here set  $n=0,1,\cdots,N-1$  for  $d_{n,k}$  and  $d_{0,k}=x_k$  to include the case that there is one sub-channel which is required to transmit the reference chaotic chip. More explicitly, when n=0,  $d_{0,k}$  denotes the kth reference chaotic chip, while when  $1 \le n \le N-1$ ,  $d_{n,k}$  denotes the information bearing chaotic chips  $d_{n,k}=s_nx_k$ .

Then the elements of  $d_{n,k}$  with all n and k are sent to the frequency hopping module and hop randomly in the frequency domain as follows.

2) Frequency hopping: In the frequency hopping module, the input symbols  $d_{n,k}$  hop randomly and non-repetitively, then we obtain the output symbols denoted by  $d'_{n,k}$  under the assumption that the length of the chaotic sequence equals to the subcarrier number, i.e.,  $\beta = N$ .

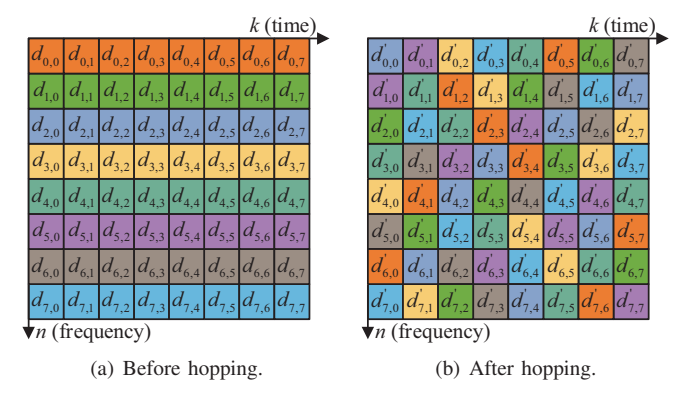


Fig. 2. The illustration of the distributions of the chaotic symbols in the time domain and in the frequency domain before and after the frequency hopping. N=8 and  $\beta=8$ .

Fig. 2 illustrates the distributions of the reference chaotic chips and the information-bearing chaotic modulated chips in the time domain and the frequency domain when  $\beta=N=8$ . In Fig. 2, each color block refers to one chip of chaotic sequences, and blocks with different colors correspond to different chaotic sequences. Namely, each chaotic sequence is respectively and non-repetitively transmitted over one single subcarrier before the frequency hopping operations, while after the hopping all chips in one chaotic sequences are hopped to all subcarriers.

Next, we derive the frequency hopping matrix to analytically express the hopping operations. We define the frequency hopping operation as a matrix denoted by  $\mathbf{U}$ .

Firstly, the chips are collected in every  $\beta$  time slot before the hopping operation. The matrix constructed by the input chips are denoted by  $\mathbf{D} = [\mathbf{d_0^T}, \mathbf{d_1^T}, \cdots, \mathbf{d_k^T}, \cdots, \mathbf{d_{\beta-1}^T}]$ , where  $(\cdot)^T$  denotes the transposition and  $\mathbf{d_k} = [d_{0,k}, d_{1,k}, \cdots, d_{n,k}, \cdots, d_{N-1,k}]$ .

Then the hopping operations can be expressed as [13]

$$\mathbf{d_{n}^{'}} = \mathbf{d_{k}U_{k}} \tag{2}$$

where  $U_k$  denotes the hopping matrix corresponding to the kth chaotic sequence  $d_k$ , n = k, which determines

the hopping pattern,  $\mathbf{d_n'} = [d_{n,0}', d_{n,1}', \cdots, d_{n,k}', \cdots, d_{n,\beta-1}']$  is the nth chaotic sequence which constitutes  $\mathbf{D'} = [\mathbf{d_0'}^T, \mathbf{d_1'}^T, \cdots, \mathbf{d_n'}^T, \cdots, \mathbf{d_{N-1}'}^T]^T$ .

Notably, the hopping matrix  $\mathbf{U_k}$  has only one "1" in each row and each column. When the random hopping pattern is employed, the position of element "1" will be randomly distributed. Meanwhile,  $\mathbf{U_k}$  has the constraint that the result of  $\sum_{k=0}^{\beta-1} \mathbf{U_k}$  is the matrix whose all elements are "1". For example, in another case that the cyclic hopping pattern is employed, then according to [13],  $\mathbf{U_k}$  is defined as

$$\mathbf{U_k} = \begin{bmatrix} \mathbf{0} & \mathbf{E_{g_k}} \\ \mathbf{E_{N-g_k}} & \mathbf{0} \end{bmatrix} \tag{3}$$

where  $\mathbf{E_{g_k}}$  is the  $g_k \times g_k$ -dimension identity matrix and  $\mathbf{E_{N-g_k}}$  is the  $(N-g_k) \times (N-g_k)$ -dimension identity matrix.

As suggested by our previous work in [14], we can generate the dimension  $g_k$  in Eq. (3) using the chaotic scrambling method. Namely, let  $\mathbf{c_m} = [c_{m,0}, c_{m,1}, \cdots, c_{m,N-1}]$  denote the chaotic sequence used to determine the hopping pattern. Then  $g_k$  can be generated with  $\mathbf{c_m}$  using the method given in [14].

In general, no matter what the hopping pattern is employed, for each chip in the chaotic sequence, we can rewrite the frequency hopping operations based on Eq. (2) as

$$d_{n,k} = d'_{k,f(n,k)} \tag{4}$$

where f(n,k) determines the hopping pattern. Take the cyclic hopping pattern as an example, for the nth chaotic modulated symbol and the kth chaotic chip, f(n,k) can be written as  $f(n,k) = (n+g_k) \mod \beta$ , where mod is the modulo operation.

From Eq. (2)-Eq. (4), we can see that the frequency hopping module guarantees that the chaotic chips from all chaotic sequences over each subcarrier are transmitted in different and random time slots. Therefore, when we transmit user data over the frequency selective channel, the frequency diversity can be fully exploited for the information reception and different CFR of every subcarrier can be figured out.

3) OFDM modulation: After the frequency hopping, the IFFT operations are performed on  $d'_{n,k}$  as below

$$s_{i,k} = \frac{1}{\sqrt{N}} \sum_{n=0}^{N-1} d'_{n,k} e^{\frac{2\pi\psi(n)i}{N}}$$
 (5)

where N is the number of subcarrier, k is the index of chaotic chip time slot,  $\psi(n)$  is the subcarrier index for the nth data stream, where  $0 \leq \psi(n) \leq N_l - 1$  and  $N_l > N$  is the total subcarrier number, i is the index of IFFT-modulated symbols in a chip time slot.

Then the OFDM symbols are transmitted over the channels after carrying out the P/S conversions and adding the CP.

#### B. NC-FH-OFDM-DCSK Receiver Structure

Fig. 3 illustrates the NC-FH-OFDM-DCSK receiver. After the S/P conversion and the CP removal, the received data symbols are sent to the fast Fourier transform (FFT) module for OFDM demodulations, then the information-bearing data symbols are extracted base on the spectrum map and are delivered to the frequency de-hopping module to recover

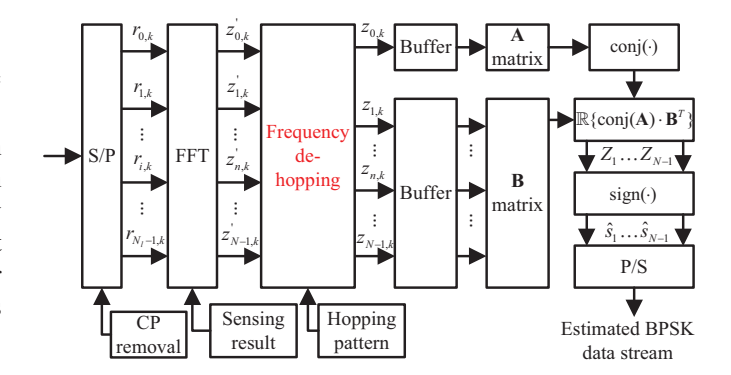


Fig. 3. The NC-FH-OFDM-DCSK receiver structure.

the original chaotic modulated symbols sequentially. The dehopped symbols are saved in buffers and are sequentially chosen in every  $\beta$  symbol to perform the correlation demodulation. Finally, the maximum likelihood detection is applied to estimate information symbols. More detailed descriptions about the information recovery operations carried out in the receivers are presented as below.

1) OFDM demodulation: At the receiver, after the FFT, the received symbol  $z_{n,k}^{'}$  over the nth subcarrier corresponding to the kth chaotic chip is denoted by

$$z'_{n,k} = \frac{1}{\sqrt{N_l}} \sum_{i=0}^{N_l - 1} r_{i,k} e^{-\frac{2\pi n i}{N}} = H_{n,k} d'_{n,k} + \xi_{n,k}$$
 (6)

where  $r_{i,k}$  denotes the received data symbol over the nth subcarrier corresponding to the ith chaotic chip,  $\xi_{n,k}$  is the complex Gaussian noise with zero mean and power spectral density of  $N_0$ ,  $H_{n,k}$  is the actual CFR over the nth subcarrier corresponding to the kth chip. In the special case that transmitted data experience the flat fading, i.e., the CFR remains constant in the time domain, we have  $H_{n,k} = H_n$  for  $\forall k$ .

2) Frequency de-hopping: Then the frequency de-hopping operations reverse to the hopping at the transmitter are performed on the OFDM demodulated symbols. For the receivers, the de-hopping matrix is known before the transmission of user data, which can be learned via the specific control channel or via some secure uncoordinate transmissions [15].

Considering the assumptions that  $\beta=N$  at the transmitter, according to Eq. (8) and similar to Eq. (2), given  $\mathbf{Z}'=[\mathbf{z_0^{'}}^T,\mathbf{z_1^{'}}^T,\cdots,\mathbf{z_n^{'}}^T,\cdots,\mathbf{z_{N-1}^{'}}^T]^T$  and  $\mathbf{z_n^{'}}=[z_{n,0}^{'},z_{n,1}^{'},\cdots,z_{n,k-1}^{'}]$ , in the case that the cyclic hopping pattern is employed, the frequency de-hopping can be derived as

$$\mathbf{z_k} = \mathbf{z_n'} \mathbf{U_k}^{-1} \tag{7}$$

where n=k,  $\mathbf{U_k}^{-1}$  is the inverse matrix of  $\mathbf{U_k}$ , the resultant vector after the de-hopping operations is  $\mathbf{z_k} = [z_{0,k}, z_{1,k}, \cdots, z_{n,k}, \cdots, z_{N-1,k}]$  and  $\mathbf{Z} = [\mathbf{z_0}^T, \mathbf{z_1}^T, \cdots, \mathbf{z_k}^T, \cdots, \mathbf{z_{\beta-1}}]$ .

Similar to the discussions for the hopping operations mentioned above, in the general case that a random hopping pattern is used, the de-hopping operations can be expressed as

$$z_{n,k} = z'_{k,f(n,k)} (8)$$

where f(n,k) has the same expression as the one given above. 3) Detection and estimation: After the frequency dehopping, the obtained reference chaotic chips from different

chaotic sequences are stored by buffers. Next, the correlated demodulations are performed on the reference chaotic sequence and information bearing chaotic sequences, then we can obtain the nth information symbol by calculating

$$Z_n = \Re\left\{\sum_{k=0}^{\beta-1} z_{0,k}^* \cdot z_{n,k}\right\}$$
 (9)

where  $\Re\{\cdot\}$  takes the real part of signal,  $(\cdot)^*$  represents the conjugation operation and  $z_{0,k}$  is the kth element of the reference chaotic sequence.

Finally, the estimation of the transmitted symbols, which is denoted by  $\hat{s}_n$ , can be obtained as  $\hat{s}_n = \operatorname{sgn}(Z_n)$ , where  $\operatorname{sgn}(\cdot)$  is the sign function.

Notably, it can be seen from Eq. (6) and Eq. (9) that no CSI estimations are required for the information retrieval. Hence with our NC-FH-OFDM-DCSK design, we can recover the information by utilizing the frequency diversity and the ergodic property of wireless channels, which means that the presented NC-FH-OFDM-DCSK scheme can effectively combat the frequency selective fading, which would be verified via the following theoretical analysis and the simulation results.

# III. PERFORMANCE ANALYSIS

In this section, we will analyze BER performances of NC-FH-OFDM-DCSK.

Assuming that  $\beta$  is large enough and the channel remains constant in the time domain. Using Gaussian approximation (GA) [16], we can derive the theoretical BER expressions over wireless channels, including AWGN channel, flat fading channel and frequency selective Rayleigh fading channel.

Firstly, we derive the received de-hopped symbols by using Eq. (4), Eq. (6) and Eq. (8) as

$$z'_{k,f(n,k)} = z_{n,k} = H_{k,f(n,k)} d'_{k,f(n,k)} + \xi_{k,f(n,k)}$$

$$= H_k d_{n,k} + \xi_{k,f(n,k)}$$
(10)

where  $z_{0,k}$  denotes the reference chaotic chip when n=0, when  $n\geq 1$ ,  $z_{n,k}$  is the information-bearing modulated chip,  $H_k$  is the complex and time-invariant CFR with zero mean and power spectral density of 1 and  $\xi_{k,f(n,k)}$  is the noise after the hopping, which has the same mean and variance as  $\xi_{n,k}$ .

Then, according to Eq. (9) and Eq. (10), we can derive the demodulated symbol  $Z_n$  for  $n \ge 1$  as

$$Z_{n} = \Re\left\{ \sum_{k=0}^{\beta-1} (H_{k} d_{0,k} + \xi_{k,f(0,k)})^{*} (H_{k} d_{n,k} + \xi_{k,f(n,k)}) \right\}$$

$$= \Re\left\{ \sum_{k=0}^{\beta-1} s_{n} |H_{k}|^{2} x_{k}^{2} \right\} + \Re\left\{ \sum_{k=0}^{\beta-1} \xi_{k,f(0,k)}^{*} \xi_{k,f(n,k)} \right\}$$

$$+ \Re\left\{ \sum_{k=0}^{\beta-1} (H_{k}^{*} x_{k} \xi_{k,f(n,k)} + s_{n} H_{k} x_{k} \xi_{k,f(0,k)}^{*}) \right\}$$

$$P_{3}$$

$$(11)$$

where  $P_1$  contains the desired signal, while  $P_2$  and  $P_3$  are the disturbance components. Due to the statistical independence

of  $P_1$ ,  $P_2$  and  $P_3$ , the expectation and variance of  $Z_n$  can be easily calculated by

$$E\{Z_n|(s_n = \pm 1)\} = \sum_{w=1}^3 E\{P_w|(s_n = \pm 1)\}$$

$$var\{Z_n|(s_n = \pm 1)\} = \sum_{w=1}^3 var\{P_w|(s_n = \pm 1)\}$$
(12)

where  $E\{\cdot\}$  denotes the expectation operator and  $\mathrm{var}\{\cdot\}$  takes the variance. According to Eq. (12), the signal-to-noise-plus-interference ratio (SINR) expression can be obtained as  $\Gamma = (E\{Z_n | (s_n = \pm 1\})^2/\mathrm{var}\{Z_n | (s_n = \pm 1)^2/\mathrm{var}\{Z_n | (s_n = \pm 1)$ 

In order to give a more informative BER equation, using the central limit theorem, the statistical characteristics of  $P_1$ ,  $P_2$  and  $P_3$  are determined with zero mean and unit power spectral density of  $H_k$  by

$$\begin{aligned}
& \mathbb{E}\{P_{1}|s_{n} = +1\} = -\mathbb{E}\{P_{1}|s_{n} = -1\} = \beta \mathbb{E}\{x_{k}^{2}\} \\
& \mathbb{E}\{P_{2}|s_{n} = \pm 1\} = \mathbb{E}\{P_{3}|s_{n} = \pm 1\} = 0 \\
& \text{var}\{P_{1}|s_{n} = \pm 1\} = \beta \text{var}\{x_{k}^{2}\} \\
& \text{var}\{P_{2}|s_{n} = \pm 1\} = \frac{1}{2}\beta N_{0}^{2} \\
& \text{var}\{P_{3}|s_{n} = \pm 1\} = \beta \mathbb{E}\{x_{k}^{2}\}N_{0}.
\end{aligned} \tag{13}$$

Finally the BER of NC-FH-OFDM-DCSK over frequency selective Rayleigh fading channel can be derived as

$$BER_{Selective} = \operatorname{erfc}(\sqrt{\Gamma/2})/2$$

$$= \frac{1}{2}\operatorname{erfc}\left[\left(\frac{1}{\beta} + \frac{2NN_0}{E_b(N-1)} + \frac{N^2N_0^2\beta}{E_b^2(N-1)^2}\right)^{-\frac{1}{2}}\right]$$
(14)

where  $E_b = N\beta E\{x_k^2\}/(N-1)$  is the average bit energy.

It is noticeable that from Eq. (14), we can observe that the BER of NC-FH-OFDM-DCSK is not related with CFR. Namely, in our presented NC-FH-OFDM-DCSK, the channel responses over each subcarrier have been embedded into the chaotic chips, thus the CSI and the corresponding channel estimation operations are no longer required.

Furthermore, similar to Eq. (13) and Eq. (14), the BER over AWGN channel and flat Rayleigh fading channel can be derived as

$$BER_{AWGN} = BER_{Flat}$$

$$= \frac{1}{2} \operatorname{erfc} \left[ \left( \frac{1}{\beta} + \frac{2NN_0}{E_b(N-1)} + \frac{N^2 N_0^2 \beta}{E_b^2 (N-1)^2} \right)^{-\frac{1}{2}} \right].$$
 (15)

From Eq. (14) and Eq. (15), we can see that the BER expressions over the AWGN channel, the flat fading channel and the frequency selective fading channels are similar to each other since no CFR is required. Thus the BER of the presented NC-FH-OFDM-DCSK system will remain similar no matter what statistical characteristics of wireless channels.

By contrast, in conventional OFDM-DCSK systems [9], the receivers require the exact CSI for information recovery and BER is dependent on the CSI estimation precision, hence the imperfect CSI estimation in practical systems will significantly degrade the BER performances. Thus, the conventional OFDM-DCSK systems will have worse reliability performance than the presented NC-FH-OFDM-DCSK system, which will be verified by the simulation results given in Section IV.

#### IV. SIMULATION RESULTS

In this section, simulations on BER performance is provided. Besides, we will compare the performances of NC-FH-OFDM-DCSK system with the ones of conventional OFDM-DCSK [9] systems.

# A. BER Performances of NC-FH-OFDM-DCSK System

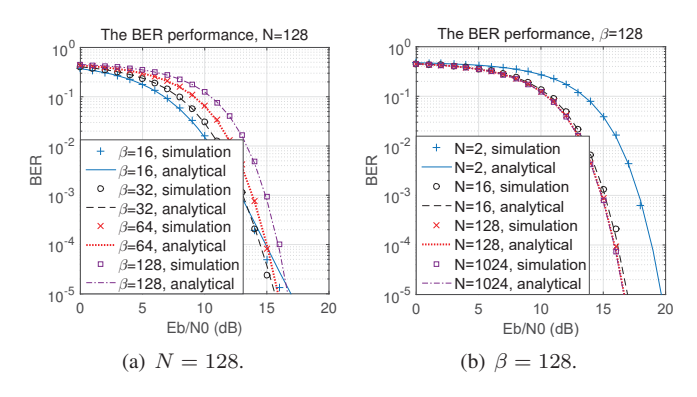


Fig. 4. The theoretical and simulated BER performances of NC-FH-OFDM-DCSK system over frequency selective Rayleigh fading channel.

Firstly, in Fig. 4(a), we demonstrate that the theoretical BER match the simulated BER performance of the NC-FH-OFDM-DCSK system over frequency selective Rayleigh fading channel when  $\beta=16,32,64,128$ , which verifies the effectiveness of our derivations.

Secondly, Fig. 4(b) also verifies that the effectiveness of our derivations. Besides, it can be observed from Fig. 4(a) and Fig. 4(b) that the BER performances of NC-FH-OFDM-DCSK system become better for larger subcarrier number N and smaller chaotic sequence length  $\beta=128$ . When N is larger than 16, the BER performances are weakly related to N, which is in accordance with the theoretical result given by Eq. (14) that the value of N/(N-1) is close to 1.

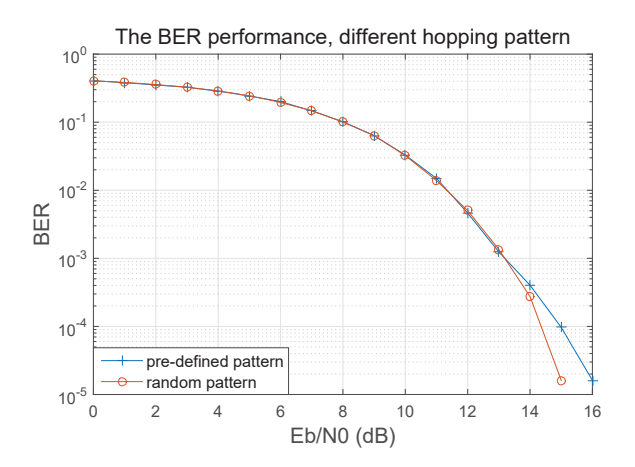


Fig. 5. The BER performances of NC-FH-OFDM-DCSK system over frequency selective Rayleigh fading channel when difference hopping pattern is employed.

Then we investigate the influence of the hopping pattern on the BER performance in Fig. 5, where the pre-defined pattern represents that the hopping pattern remains unchanged during the transmissions of the information symbols, while the random hopping pattern means that every NC-FH-OFDM-DCSK symbol hops with different hopping patterns. It can be observed that the BER performances are almost unrelated with the hopping pattern settings.

# B. BER Performance Comparisons of NC-FH-OFDM-DCSK and OFDM-DCSK Systems

For fairness of performance comparisons, the same parameter settings are employed for the compared systems. Then we compare the BER performances of the NC-FH-OFDM-DCSK system with the counterpart OFDM-DCSK systems [9] and OFDM-CS-DCSK systems [17] with imperfect CSI.

The imperfect CSI is obtained via channel estimation module as [18], [19]

$$\hat{H}_{n,k} = \rho H_{n,k} + \sqrt{1 - \rho^2} \epsilon_{n,k} \tag{16}$$

where  $\hat{H}_{n,k}$  is the estimated CFR,  $H_{n,k}$  is the actual CFR with zero mean and unit power spectral density, the estimation error  $\epsilon_{n,k}$  is a Gaussian random variable independent from  $H_{n,k}$  and has 0 mean and the variance of  $\sigma_e^2$  which equals to the power of errors, and the correlation coefficient  $\rho$  determines the quality of channel estimations.

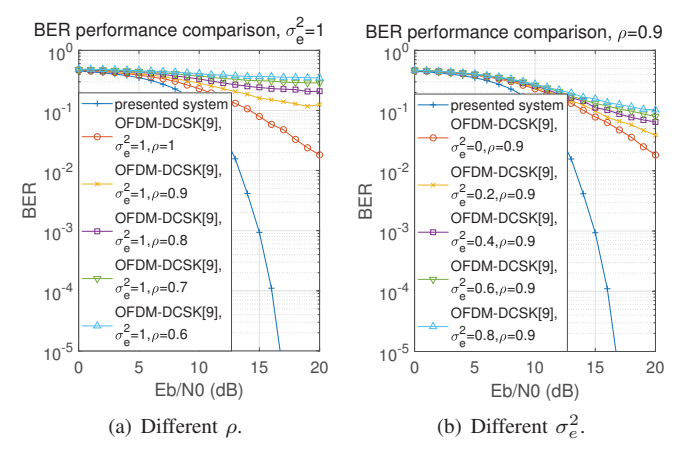


Fig. 6. The BER performance comparison of the NC-FH-OFDM-DCSK system and the OFDM-DCSK system [9] over single path frequency selective fading channels when N=128 and  $\beta=128$ .

We firstly compare the BER performances of the presented NC-FH-OFDM-DCSK system without channel estimation and the OFDM-DCSK system [9] with different channel estimation precisions such as various  $\rho$  and  $\sigma_e^2=1.$  From Fig. 6(a), we can observe that for lower channel estimation precision corresponding to smaller  $\rho$ , the BER performances of OFDM-DCSK systems become worse. By contrast, the presented NC-FH-OFDM-DCSK system achieve better performances than the OFDM-DCSK systems even when  $\rho=1$  which means that the exact CSI is provided for the receivers. Thus, thanks to the frequency hopping in our design, more reliable performance can be provided for the systems with imperfect CSI.

Then we evaluate the influence of the channel estimation error on the BER performance when  $\rho$  is fixed as  $\rho=0.9$ . As illustrated in Fig. 6(b), it can be observed that the BER performances of OFDM-DCSK systems become worse when the power of the estimation error gets higher, while the BER

performances of NC-FH-OFDM-DCSK system are better then those of OFDM-DCSK systems, even in the case that exact CSI can be obtained at the receiver, i.e,  $\sigma_e^2 = 0$ .

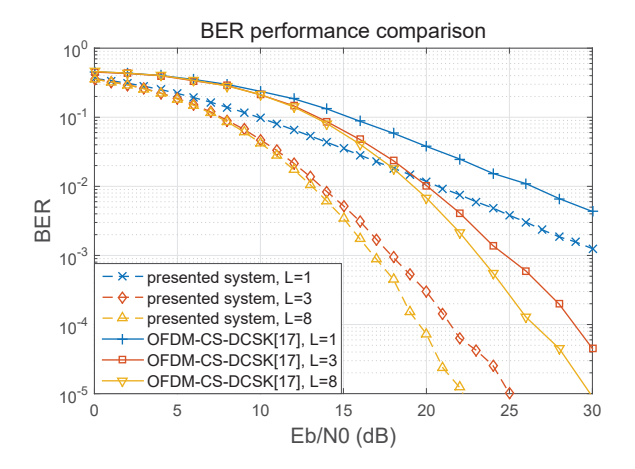


Fig. 7. The BER performance comparison of the NC-FH-OFDM-DCSK system and the OFDM-CS-DCSK system [17] over multi-path frequency selective fading channels when  $N\beta=64$ .

Subsequently, we compare the BER performances of the NC-FH-OFDM-DCSK system and the OFDM-CS-DCSK system [17] over multi-path frequency selective fading channels, where L denotes the channel path number. In the simulation, each channel path has the average power of  $\mathrm{E}\{(h_l^2)\}=\mathrm{E}\{(h_l^2)\}e^{-\epsilon(l-1)}$  for  $l=1,2,\cdots,L$ , the power decay factor of  $\epsilon=1$  and the summed average power of  $\sum_{l=1}^L\mathrm{E}\{(h_l^2)\}=1$  [17]. The length of CP is 8.

It can be seen from Fig. 7 that the presented NC-FH-OFDM-DCSK system achieves better BER performances over multipath frequency selective Rayleigh fading channels. When L increases, better BER performances can be achieved. Moreover, the NC-FH-OFDM-DCSK system can obtain better BER performances than the counterpart OFDM-CS-DCSK systems thanks to the diversity provided by the frequency hopping.

# V. CONCLUSION

In this paper, we propose the NC-FH-OFDM-DCSK scheme to enhance both the reliability performance. By exploiting the frequency diversity provided by the frequency hopping, the chips from all chaotic sequences hop randomly and will be transmitted over different subcarriers in different time slots. Thus the CFR of each sub-channel is naturally embedded into the chaotic chips and then used for information recovery in the receivers. Hence the requirement for exact CSI is removed, and the presented NC-FH-OFDM-DCSK scheme can be used for practical communication systems with imperfect CSI. Furthermore, the theoretical BER is derived, which have been verified to be effective by the simulations. Moreover, the simulations under different parameter settings demonstrate that the presented NC-FH-OFDM-DCSK system can achieve better BER performances than counterpart schemes over frequency selective Rayleigh fading channels, thereby better reliability performance has been attained by applying our design. Moreover, the presented NC-FH-OFDM-DCSK design can effectively enable the high data rate CR or CA systems to provide reliable transmission services over contiguous or NC bands without requiring CSI.

#### VI. ACKNOWLEDGEMENTS

This work was supported by the National Natural Science Foundation of China under Grant (No. 61602531), partially supported by the Opening Project of Guangdong Province Key Laboratory of Information Security Technology(Grant No. 2017B030314131), NSF grant 1748494 and OFRN. The authors want to thank Prof. Lin Wang and Prof. Weikai Xu for their invaluable support.

#### REFERENCES

- [1] A. Ghosh, R. Ratasuk, B. Mondal, N. Mangalvedhe, and T. Thomas, "LTE-advanced: next-generation wireless broadband technology [invited paper]," *IEEE Wireless Commun.*, vol. 17, no. 3, pp. 10–22, June 2010.
- [2] X. Hong, J. Wang, C. Wang, and J. Shi, "Cognitive radio in 5G: a perspective on energy-spectral efficiency trade-off," *IEEE Communications Magazine*, vol. 52, no. 7, pp. 46–53, July 2014.
- [3] D. Cabrić, S. M. Mishra, D. Willkomm, R. Brodersen, and A. Wolisz, "A cognitive radio approach for usage of virtual unlicensed spectrum," in 14th IST Mobile and Wireless Communications Summit, Dresden, Germany, Jun. 2005.
- [4] F. C. M. Lau and C. K. Tse, Chaos-Based Digital Communication Systems. New York, NY, USA: Springer, 2003.
- [5] G. Kaddoum and N. Tadayon, "Differential chaos shift keying: A robust modulation scheme for power-line communications," *IEEE Trans. Circuits Syst. II, Exp. Briefs*, vol. 64, no. 1, pp. 31–35, Jan 2017.
- [6] G. Kolumbán, B. Vizvári, W. Schwarz, and A. Abel, "Differential chaos shift keying: A robust coding for chaos communication," in *Proc.* NDES'96, 1996, pp. 87–92.
- [7] Y. Fang, G. Han, P. Chen, F. C. M. Lau, G. Chen, and L. Wang, "A survey on DCSK-based communication systems and their application to UWB scenarios," *Commun. Surveys Tuts.*, vol. 18, no. 3, pp. 1804–1837, thirdquarter 2016.
- [8] G. Kaddoum, F. D. Richardson, and F. Gagnon, "Design and analysis of a multi-carrier differential chaos shift keying communication system," *IEEE Trans. Commun.*, vol. 61, no. 8, pp. 3281–3291, Aug. 2013.
- [9] S. Li, Y. Zhao, and Z. Wu, "Design and analysis of an OFDM-based differential chaos shift keying communication system," *J. Commun.*, vol. 10, no. 3, pp. 199–205, Mar. 2015.
- [10] H. Schulze and C. L\u00fcders, Theory and applications of OFDM and CDMA: Wideband wireless communications. John Wiley & Sons, 2005.
- [11] W. Hu, L. Wang, G. Cai, and G. Chen, "Non-coherent capacity of M-ary DCSK modulation system over multipath rayleigh fading channels," IEEE Access, vol. 5, pp. 956–966, 2017.
- [12] A. Kumar, P. R. Sahu, and J. Mishra, "Performance analysis of DCSK modulation with diversity combining not requiring channel state information," in 2016 Twenty Second National Conference on Communication (NCC), March 2016, pp. 1–6.
- [13] T. Scholand, T. Faber, A. Seebens, P. Jung, J. Lee, J. Cho, Y. Cho, and H. W. Lee, "Fast frequency hopping OFDM concept," *Electron. Lett.*, vol. 41, no. 13, pp. 748–749, June 2005.
- [14] H. Lu, L. Zhang, M. Jiang, and Z. Wu, "High-security chaotic cognitive radio system with subcarrier shifting," *IEEE Commun. Lett.*, vol. 19, no. 10, pp. 1726–1729, 2015.
- [15] B. Chen, L. Zhang, and H. Lu, "High security differential chaos-based modulation with channel scrambling for WDM-aided VLC system," *IEEE Photon. J.*, vol. 9, no. 5, 2016.
- [16] Y. Xia, C. K. Tse, and F. C. M. Lau, "Performance of differential chaos-shift-keying digital communication systems over a multipath fading channel with delay spread," *IEEE Trans. Circuits Syst. II, Exp. Briefs*, vol. 51, no. 12, pp. 680–684, Dec 2004.
- [17] M. Chen, W. Xu, D. Wang, and L. Wang, "Design of a multi-carrier different chaos shift keying communication system in doubly selective fading channels," in 2017 23rd Asia-Pacific Conference on Communications (APCC), Dec 2017, pp. 1–6.
- [18] B. Prasad, S. D. Roy, and S. Kundu, "Outage and SEP of secondary user with imperfect channel estimation and primary user interference," in 2014 IEEE International Conference on Electronics, Computing and Communication Technologies (CONECCT), Jan 2014, pp. 1–6.
- [19] A. Pascual-Iserte, D. P. Palomar, A. I. Perez-Neira, and M. A. Lagunas, "A robust maximin approach for MIMO communications with imperfect channel state information based on convex optimization," *IEEE Trans. Signal Process.*, vol. 54, no. 1, pp. 346–360, Jan 2006.